

Copyright is owned by the Author of the thesis. Permission is given for a copy to be downloaded by an individual for the purpose of research and private study only. The thesis may not be reproduced elsewhere without the permission of the Author.

**Physico-Chemical Characterisation and Functionality of the
Polysaccharide Extracted from the New Zealand Black Tree
Fern, *Cyathea medullaris* (Mamaku)**



A thesis presented in partial fulfilment of the requirements for the degree of

Doctor of Philosophy

in

Food Technology

At Massey University, Palmerston North, New Zealand

May Wee Sui Mei

2015

Preface

What do the New Zealand black tree fern and the Russian Matroyshka doll have in common?

The Matroyshka doll is a doll in a doll in a doll. And the tree fern? It is but a fern in a fern in a fern. The fronds make up the fern tree, which is made up of smaller frond representations called the primary pinna, which is made up of the secondary pinna, which is, (you guessed it) made up of the tertiary pinna. Looking at the tertiary pinna is no different from looking at the secondary, or the primary pinna. In other words, the fern is constructed of self-similar shapes. The figure below is an actual tertiary pinna of the black tree fern scanned as an image. It looks just like an entire fern leaf blade doesn't it?

*This self-similarity or macrocosmic characteristic of nature is seemingly random and sometimes oblivious to the human mind trained by classical geometry. To Benoit Mandelbrot, the recursive nature of the tree fern is what he came to describe as **fractals** in 1977. Fractals are a family of shapes, characterised by irregularities and self-similarity which are still statistical in nature. Triangles, squares and circles are shapes, as much as flowers, snowflakes, clouds, waves and even Brownian motion can be.*

Keeping in mind that fractals are the underlying fundamentals of nature can prepare us to recognise the order within the disorder, and not be bound by current knowledge. For every researcher dealing with nature, there is always one thing to remember: God might not play dice, but it will most certainly play hide-and-seek. It is now for us to embark on a journey to seek out what wonders might lie within the polysaccharide extracted from the New Zealand black tree fern in this thesis.

May 2014



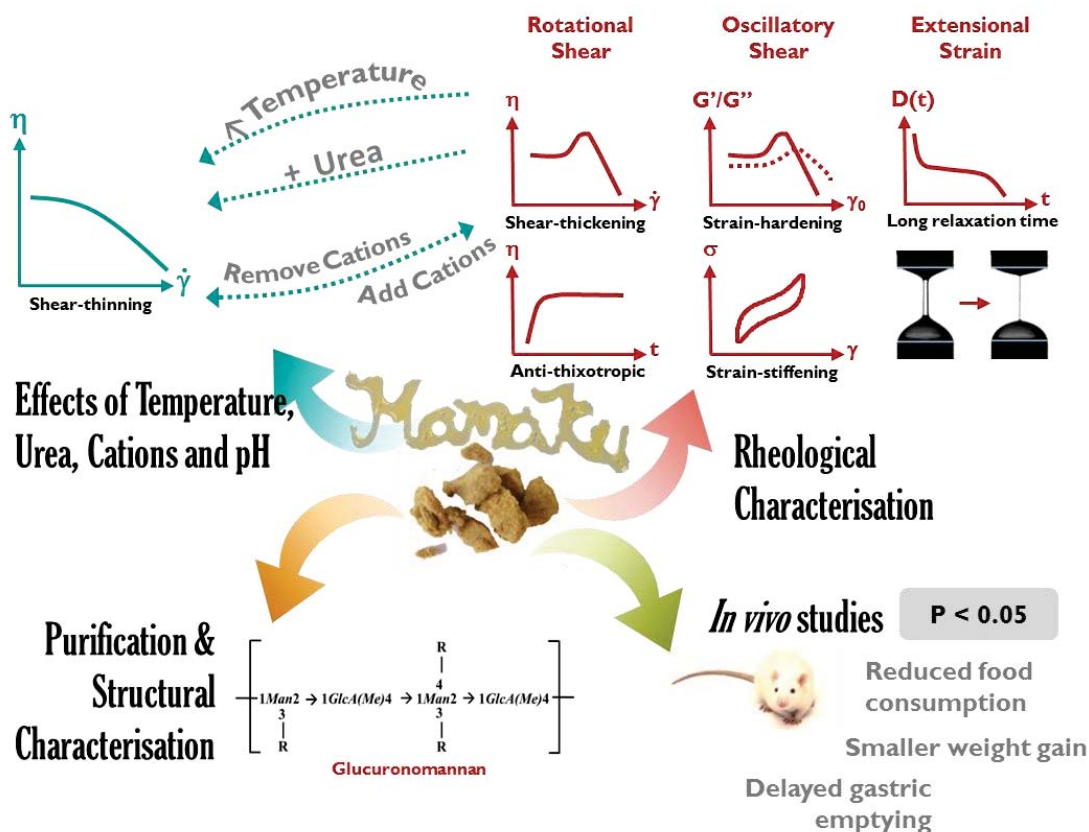
"I don't know what I'm looking for."

"Why not?"

*"Because ... because ... I think it might be because if I knew
I wouldn't be able to look for them."*

- Douglas Adams, Hitchhiker's Guide to the Galaxy

Abstract



The aim of this thesis was to characterise the polysaccharide extracted from the New Zealand black tree fern, *Cyathea medullaris*, or mamaku in Māori using a combination of rheological, structural and *in vivo* research techniques. Polysaccharides are biopolymers with diverse functionalities that have found their way into many applications in the food, cosmetic or pharmaceutical industries. Novel sources of polysaccharides may have promising functional properties for new or existing applications, therefore it is essential to have fundamental knowledge of their properties. The native and endemic New Zealand black tree fern produces mucilage (containing the polysaccharide) which is extracted from the thick fleshy stem pith of the frond.

Rheological properties of the polysaccharide were characterised using rotational shear, oscillatory shear, and extensional rheology. The combination of these techniques provided information on how the polysaccharide deformed under shear, strain and extension. Rotational shear was further classified into tests for shear-dependent viscosity/normal stresses, time-dependent viscosity, and shear-history dependent viscosity. The polysaccharide (5% w/w) exhibited shear-thickening ($4\text{-}10\text{s}^{-1}$), positive first normal stress differences coinciding with shear-thickening, anti-thixotropy (under constant shear with time at shear rates between $4\text{-}10\text{s}^{-1}$), and thixotropy (at 1s^{-1} , pre-sheared at 10s^{-1}) or rheopexy (at 10s^{-1} , pre-sheared at 1000s^{-1}) depending on shear-history. Oscillatory shear was classified into linear and nonlinear rheology, *i.e.* small amplitude (SAOS) and large amplitude oscillatory shear (LAOS) respectively. Under linear strain deformation, the polysaccharide displayed viscoelasticity and a power-law dependence on concentration for relaxation time ($\lambda_s \sim c^{3.6}$). Complex viscosity did not superimpose on shear viscosity at higher shear rates/angular frequency (nonlinear region),

therefore not complying with the Cox-Merz rule. The LAOS response in the nonlinear region was characterised by new large-strain and minimum-strain moduli parameters (G'_L and G'_M), as well as the traditional first-harmonic storage modulus G' . The polysaccharide (10% w/w mamaku) was found to exhibit first a linear viscoelastic region (0.1-20% γ_0), followed by strain-softening (20-800% γ_0), then strain hardening (800-2000% γ_0) and finally a second strain-softening region due to viscous flow (>2000% γ_0) for all three elastic moduli measurements. Closer examination of Lissajous plots in the intercycle strain-hardening region revealed deviation from ellipsoidality *i.e.* sigmoidal shapes, which were representative of intracycle strain-stiffening. Finally, the evolution of filament diameter with time and extensional relaxation time were characterised using a capillary breakup extensional rheometer (CaBER). The polysaccharide exhibited long extensional relaxation times (4.6s), high extensional viscosities ($\sim 10^4$) and large Trouton ratios ($\sim 10^4$).

Factors *i.e.* temperature, urea concentration, cations (ionic strength) and pH were tested to investigate how changes in the environment would affect the rheological properties of the polysaccharide. These factors are also intrinsically related to intermolecular interactions which may be present in the polysaccharide *e.g.* hydrogen bonding, hydrophobic interaction and electrostatic attractions. Thus the molecular origin of its rheological behaviour could also be elucidated through these effects. Shear-thickening was lost at higher temperatures ($\geq 50^\circ\text{C}$) but enhanced at low temperatures. The peak viscosity during shear-thickening exhibited an Arrhenius' Law dependency with an activation energy of flow of ~ 90 kJ/mol (5% w/w). Hydrogen bonds are sensitive to temperature and inversely proportion to temperature in the order of kT , which indicated that hydrogen bonds are likely to be involved in shear-thickening of the polysaccharide. The addition of urea, a hydrogen-bond disruptor (chaotropic agent) suppressed shear-thickening completely in 5% w/w mamaku solution at a concentration of 5M. Urea molecules compete for hydrogen bonding sites with the polysaccharide and lower the lifetime of polymer-polymer associations. Removal of salts from the native mamaku solution via dialysis resulted in loss of shear-thickening as well. However, shear-thickening was reinstated upon addition of salts (NaCl, KCl, $\text{N}(\text{CH}_3)_4\text{Cl}$, CaCl_2 , MgCl_2 , $\text{LaCl}_3 \cdot 7\text{H}_2\text{O}$, $\text{AlCl}_3 \cdot 6\text{H}_2\text{O}$) back. Mono-, di- and trivalent cations screen the electrostatic charges on the polysaccharide thus lowering the viscosity as the polysaccharide adopts a more compact configuration. In addition, trivalent cations also cause chain collapse (precipitation) and re-dissolution of the polysaccharide, a phenomenon known as re-entrant condensation in polyelectrolytes. Lastly, shear-thickening was also recovered in the dialysed extract at pH 2-4. Similarly, the protons (H^+) screen the electrostatic charges which lowered the viscosity of the polysaccharide. Screening of electrostatic repulsion appeared to promote shear-thickening rather than ionic cross-linking, since monovalent cations and protons were able to recover shear-thickening.

Chemical structure is an important identity for any polysaccharide. In addition, the chemical structure can provide insight as to how the polysaccharide may have participated in shear-thickening. The native mamaku extract was further purified prior to structural characterisation via ultracentrifugation, starch hydrolysis, de-proteinisation and ethanol (80% w/v) precipitation. This method of purification yielded approximately 15% of purified material, removing most of the starch, minerals and simple sugars from the native extract. The purified fraction retained its shear-thickening character and had a molecular weight of 1.94×10^6 Da. Structural characterisation determining monosaccharide composition and glycosyl linkages were carried out using methylation, HPLC/GC, GC-MS and NMR techniques. The structure of the mamaku polysaccharide was

suggested to be a glucuronomannan backbone (methylesterified 4-Glc₆P₄A (27.9 mol%) with 2,3- (9.2 mol%) and 2,3,4-linked Man₆P₄ (10.9 mol%)) with branched sugar side-chains of galactose, arabinose, xylose, non-methylesterified glucuronic acid (8.2 mol%) and other simple sugars at the O-3 and O-4 of the mannose residues.

Piecing the information obtained from the various characterisation techniques together helped to elucidate the molecular origin of shear-thickening, anti-thixotropy, strain-hardening and extensional-hardening. They were postulated to be of the same event, *i.e.* intra- to intermolecular association between polysaccharide chains during shear, strain or extension via hydrogen bonding. Stretching the polysaccharide exposed associative groups within the long chain, which interacted in a cooperative zip-like manner. The hydrogen bonds were suggested to take place via the hydroxyl (-OH) groups of mannose or carbonyl/carboxyl groups (-C=O/-COOH) of the glucuronic acids.

Finally, the satiety effects of the mamaku gum were tested *in vivo* in rats. The functional ability of the polysaccharide to confer satiety was postulated to arise from its high viscosity as well as its shear-thickening behaviour, which alters gastric antrocorporeal contractions and delays gastric emptying. Oral gavage of the rats with mamaku gum (15% w/w) showed a significant reduction in short term food consumption ($p < 0.05$), smaller weight gains ($p < 0.05$), as well as prolonged gastric emptying ($p < 0.05$) as compared to rats gavaged with water. Therefore the polysaccharide could potentially be used as a satiety aid in food products.

Biopolymers which exhibit such complex rheological properties that can be easily controlled by manipulating environmental factors are rarely or never before encountered. Clearly, the mamaku polysaccharide would find its way into novel applications, starting with satiety enhancers.

Acknowledgements

A big, big thank you and a hug to my chief supervisor, Lara, (who cringes when called Dr. Lara Matia-Merino), for her mentorship, her guidance, her support and encouragement when skies are gloomy, and for keeping me in shape with BodyStep classes (one will be surprised at the number of cookies and cups of coffee one consumes while doing a PhD). I am very lucky to have her as a supervisor! The acknowledgements page does not do enough justice to my gratitude towards her, perhaps the only supervisor who would accompany a student on a trip to the dentist.

Another gargantuan big ('use simple English!', as he always says) thank you to my co-supervisor, Kelvin Goh, for being my mentor for the last six years ever since I was an undergraduate student. For all the constructive criticisms sandwiched between compliments, for the patience with putting up my occasional defiance, and for encouraging me to take up a PhD in the first place. Likewise, this acknowledgements page does not do enough justice to my gratitude towards him. I will be showing up in his office with an hour long speech one of these days (... did I just hear him groan 'oh no..' again?).

I would also like to thank Massey University for financially supporting me with the Massey University Doctoral Scholarship and Universities New Zealand for awarding me with the Claude McCarthy Fellowship which made my trip to MIT possible.

Thank You To my favourite lab managers who have been like friends to me, for coming to my rescue when I land myself in yet another mess, and for forgiving when my experiments start growing mould in their labs: Garry Radford, Warwick Johnson (Papa Warwick), Michelle Tamehana, Chris Hall (Edwardo) and Janiene (Flossy).

Thank You To all Massey staff who has provided so much help in the laboratories, technical issues, administrative work and the occasional chit-chat: Steve Glasgow, Julia Good, John Edwards, Michelle McGrath, Richard Haverkamp, Graham Freeman, Mark Waterland, Shane Telfer, Fliss Jackson, Gary Mack, Pat Edwards, Matt Levin, Peter Jeffery, Yvonne Parkes, Denise Mist and Eteta Trueman.

Thank You To the carbohydrate chemistry team at Industrial Research Limited (IRL) for accommodating me at your laboratory, and guiding me through the highly complicated structural analysis work in 2011 and 2012: Ian Sims, Susie Carnachan and Tracy Bell.

Thank You To the Hatsopoulos Microfluidics Laboratory team at Massachusetts Institute of Technology for inspiring me with so much more than just rheology, for opening my eyes to a world and culture I never thought I would be part of. I would like to express my sincerest thanks to Gareth McKinley for collaborating with us and his warm hospitality during my stay in Boston, to Aditya Jaishankar for being such an amazing friend who constantly fascinates me with fractals and philosophy, and the rest of the HML group Sean Buhrmester, Bavand Keshavarz, Chris Dimitriou, Divya Panchanathan, Thomas Ober, Kenneth Park, Setareh Shahsavari, and Michelle.

Thank You To the rat studies team for supporting and encouraging me in spite of all the adversities faced during execution of the trial: Roger Lentle, Kim Wylie, Anne Broomfield, Corrin Hulls, Aimee Hamlin, Juliet Cayzer, and to the animal ethics committee for approving the research.

Thank You To all Massey University lecturers for their guidance, most of whom since my undergraduate days: Alistair Carr, Allan Hardacre, Brian Wilkinson, Heather McClean, Janet Weber, Jason Hindmarsh, Matt Golding, Nigel Grigg, Owen McCarthy, Richard Archer, Richard Love, Steve Flint, Michael Parker and Tuoc Trinh.

Thank You To all my friends, office mates and flatmates who contributed to what used to be a non-existent social life: Ivana (Commando Sequeira), Hayley (Bro), Jeremy (Chest Hair), Yen, Visaka, Lakshmi, Mehak, Khaizura, Bob (Boobies), Naila, Shazla, Irene, Esther, Sandra, Chalida, Ian, Jerry, Melody, Samantha, Pamela, Matthew, Anges (High Class), Wensheng, Siang Wee, Anne, Bryan, Evgeniy (Geniy), Li Mo (Momo), Grace (Ahbuji), Faith (Ah ma), Justin, Soffalina, Daisy, Seng Guan, Jordon, Anynda (Amoeba), Tian Wen, Ling Li, Qing Ping, Sheryl, Celia, Eileen, Massey University Singapore graduates and Singapore Polytechnic internship students of years 2011-2014 who were here in Palmy.

And finally,

Thank You to my family, to God, to the universe, to the rheometer for going through shear-thickening and shear-thinning with me (it was *shear* torture!), and to life, for all the bitter-sweetness so that I shall have stories to tell

Table of Contents

PREFACE	III
ABSTRACT	VII
ACKNOWLEDGEMENTS	XI
TABLE OF CONTENTS	XIII
LIST OF FIGURES	XIX
LIST OF TABLES	XXVII
LIST OF PUBLICATIONS	XXIX
CHAPTER 1 INTRODUCTION	1
CHAPTER 2 LITERATURE REVIEW	3
2.1 Polysaccharides.....	3
2.1.1 Plant Polysaccharides	4
2.2 Structural Properties of Polysaccharides.....	9
2.2.1 Monosaccharides	10
2.2.2 Glycosidic Linkages	11
2.2.3 Conformation	12
2.3 Physical and Molecular Properties of Polysaccharides	13
2.3.1 Molecular Weight and Distribution	13
2.3.2 Intrinsic Viscosity	14
2.3.3 Solubility	15
2.3.4 Concentration	15
2.4 Rheological Properties of Polysaccharides.....	16
2.4.1 Shear-dependent Viscosity	16
2.4.2 Viscoelasticity	18

2.4.3	Extensional Viscosity.....	19
2.5	Shear-Thickening Rheology.....	21
2.5.1	Associative Polymers	22
2.5.2	Shear-Thickening Mechanisms.....	22
2.6	Intermolecular Interactions in Polysaccharides	26
2.6.1	Hydrogen Bonds	26
2.6.2	Hydrophobic Interactions	27
2.6.3	Electrostatic Attractions.....	27
2.7	Applications of Polysaccharides	28
2.7.1	Satiety Effects of Polysaccharides	29
CHAPTER 3 EXPERIMENTAL TECHNIQUES.....		33
3.1	Mamaku Gum Extraction.....	33
3.2	Rheological Characterisation.....	34
3.2.1	Rotational Shear Rheology	34
3.2.2	Small Amplitude Oscillatory Shear Rheology	41
3.2.3	Large Amplitude Oscillatory Shear Rheology	43
3.2.4	Extensional Rheology.....	47
3.3	Structural Characterisation.....	50
3.3.1	Monosaccharide Composition	50
3.3.2	Linkage Analysis	51
3.3.3	Nuclear Magnetic Resonance (NMR).....	52
3.4	Animal Studies	53
3.4.1	Rats.....	53
3.4.2	Oral Gavage	54
3.4.3	Statistical Analysis.....	55
CHAPTER 4 RHEOLOGICAL CHARACTERISATION OF MAMAKU POLYSACCHARIDE		57
.....		57
4.1	Introduction	57
4.2	Materials and Methods	58
4.2.1	Rotational Shear Rheology	58

4.2.2	Oscillatory Shear Rheology.....	58
4.2.3	Extensional Rheology (CaBER)	59
4.3	Results and Discussion	60
4.3.1	Shear-Dependent Rotational Shear Rheology.....	60
4.3.2	Time-Dependent Rotational Shear Rheology.....	61
4.3.3	Small Amplitude Oscillatory Shear Rheology	69
4.3.4	Large Amplitude Oscillatory Shear Rheology	71
4.3.5	Extensional Rheology.....	80
4.4	Conclusion.....	86
CHAPTER 5 EFFECTS OF TEMPERATURE, UREA, IONIC STRENGTH AND PH.....		87
5.1	Introduction	87
5.2	Materials and Methods	89
5.2.1	Sample Preparation	89
5.2.2	Rheological Measurements.....	90
5.2.3	Relative Viscosity	91
5.2.4	Zeta-Potential	91
5.2.5	Mineral Analysis	91
5.3	Results and Discussion	92
5.3.1	Effect of Temperature	92
5.3.2	Effect of Urea.....	98
5.3.3	Effect of Ionic Strength.....	102
5.3.4	Effect of pH	114
5.3.5	Overall Discussion.....	115
5.4	Conclusion.....	116
CHAPTER 6 PURIFICATION AND STRUCTURAL CHARACTERISATION OF MAMAKU POLYSACCHARIDE.....		117
6.1	Introduction	117
6.2	Materials and Methods	119
6.2.1	Purification.....	119
6.2.2	Chemical Analysis.....	121

6.2.3	Structural Analysis.....	123
6.2.4	Size-Exclusion Chromatography-Multi-Angle Laser Light Scattering (SEC-MALLS)	126
6.2.5	Rheological Measurements.....	127
6.3	Results and Discussion	128
6.3.1	Purification.....	128
6.3.2	Composition Analysis.....	134
6.3.3	Size-Exclusion Chromatography-Multi-Angle Laser Light Scattering (SEC-MALLS) of Purified Mamaku Polysaccharide.....	135
6.3.4	Rheological Properties of Purified Mamaku Polysaccharide	135
6.3.5	Structural Analysis.....	137
6.4	Conclusion.....	142
 CHAPTER 7 PILOT STUDY ON SATIETY EFFECTS OF MAMAKU GUM IN RATS		143
7.1	Introduction	143
7.2	Materials and Methods	144
7.2.1	Animal Ethics	144
7.2.2	Preparation of Mamaku Solution	144
7.2.3	Animals and Experimental Design	144
7.2.4	Statistical Analysis.....	145
7.2.5	Pathology	146
7.2.6	Rheological Measurements.....	146
7.2.7	Bomb Calorimetry.....	146
7.3	Results	147
7.3.1	Gastric Emptying.....	147
7.3.2	Food Consumption	148
7.3.3	Body Weight.....	149
7.4	Discussion.....	151
7.4.1	Gastric Emptying.....	151
7.4.2	Food Consumption	154
7.4.3	Body Weight Gain.....	155
7.4.4	Toxicity	155
7.5	Conclusion.....	155

CHAPTER 8 OVERALL CONCLUSIONS AND RECOMMENDATIONS.....	157
8.1 Overall Conclusions.....	157
8.2 Recommendations	164
8.2.1 Future Work.....	164
8.2.2 Applications.....	166
REFERENCES.....	169
APPENDIX.....	181

List of Figures

Figure 1.1 – Flow diagram of thesis overview	2
Figure 2.1 – Picture of the New Zealand black tree fern plant (<i>Cyathea medullaris</i>)	6
Figure 2.2 – Botanical parts of the New Zealand black tree fern plant (<i>Cyathea medullaris</i>).....	7
Figure 2.3 – Chemical structures of some monosaccharides commonly found in plant polysaccharides (adapted from Izydorczyk, 2005).....	10
Figure 2.4 – Comparison of structures between L- and D-glucose (adapted from Oakenfull, 1998)	10
Figure 2.5 – Comparison of structures between α -D and β -D-glucose	11
Figure 2.6 – Torsion angles of glycosidic bond (Izydorczyk, 2005).....	11
Figure 2.7 – Geometrical representation of various glycosidic linkage types in D-glucose; a) zig-zag $\beta(1\rightarrow4)$, b) U-turn $\beta(1\rightarrow3)$, c) twisted $\beta(1\rightarrow2)$, d) zig-zag $\alpha(1\rightarrow3)$, e) zig-zag $\alpha(1\rightarrow4)$ -D-galactose, f) U-turn $\alpha(1\rightarrow4)$ (adapted from Oakenfull, 1998)	13
Figure 2.8 – Comparison between molecular weight measurement types (M_n , M_v , M_w , M_z) for a heterogeneous polysaccharide (adapted from Steve & Qi, 2005b).....	14
Figure 2.9 – Concentration regimes of polysaccharide solutions. From left: dilute, semi-dilute and concentrated (adapted from Pieter, 2003).....	16
Figure 2.10 – Typical flow curve exhibited by a shear-thinning polysaccharide(Jacques & Jean-Louis, 2004).....	17
Figure 2.11 – Typical mechanical spectrum i.e. storage (G' , —) and loss (G'' , ---) moduli with angular frequency of an entangled polymer system; τ_d : relaxation time at crossover frequency (adapted from Jacques & Jean-Louis, 2004).....	19
Figure 2.12 – Illustration of molecule under shear (weak) and extensional (strong) deformation (adapted from Padmanabhan, 2010).....	20
Figure 2.13 – Schematic viscosity curves of different shear-thickening behaviour in materials.....	21
Figure 2.14 – a) polymers with a single associative block b) polymers with two associative end blocks c) polymers with many associative groups (red: associating blocks, blue: solvophilic blocks) (adapted from Chassenieux, et al., 2011)	22
Figure 2.15 – Schematic mechanism of shear-thickening due to cross-linking during shear (adapted from Ballard, et al., 1988).....	24
Figure 2.16 – Schematic illustration of effective (●--●), free (○--○) and dangling (●--○) chains in a transient network model (adapted from S. Q. Wang, 1992)	25
Figure 2.17 – Gaussian chain (adapted from Doi & Edwards, 1988)	25
Figure 2.18 – Functional properties and applications of polysaccharides based on their rheological, structural and physiological properties.....	29
Figure 3.1 – Pictorial representation of Mamaku extraction procedure and materials.....	33
Figure 3.2 – Two-step model demonstrating relationship between shear stress and shear rate	34
Figure 3.3 – Typical viscosity curves for a Newtonian, shear-thickening and shear-thinning fluid	35
Figure 3.4 – Typical viscosity curves for a thixotropic, anti-thixotropic and time-independent fluid at a constant shear rate	35

Figure 3.5 – Three-dimensional deformation of viscoelastic material in the x, y and z-direction	36
Figure 3.6 – Weissenberg (or rod-climbing) effect of 7% w/w mamaku solution with rod rotating at ~120 rev/min (Goh, et al., 2007)	36
Figure 3.7 – Comparison between stress responses of an elastic solid, viscous liquid and viscoelastic fluid under constant strain (adapted from Trinh & Trinh, 2009)	38
Figure 3.8 – Kelvin/Voigt mechanical spring and dashpot mechanical model for viscoelastic fluid.....	38
Figure 3.9 - Centrifugal expulsion of 5% w/w mamaku sample during viscosity measurements at approximately 50s^{-1}	40
Figure 3.10 - Viscosity curves of 5% w/w mamaku obtained using the parallel plate, cone and plate and double gap geometries.....	40
Figure 3.11 - Viscosity curves of 5% w/w mamaku obtained using the parallel plate with sandpaper, without sandpaper, and with serrated plates	40
Figure 3.12 – Stress vs. strain response (left) and Lissajous plots (right) of elastic solid, Newtonian fluid and viscoelastic fluids under small oscillatory shear	41
Figure 3.13 – Comparison of stress waveforms in the linear and nonlinear viscoelastic regions as represented on an amplitude sweep.....	43
Figure 3.14 – Classification of materials into type I) strain-thinning, II) strain-hardening, III) weak strain overshoot and IV) strong strain overshoot	44
Figure 3.15 – Quantification of G'_M and G'_L from Lissajous plots in a) linear and b) nonlinear viscoelastic regions	45
Figure 3.16 – a) Elastic and b) viscous Lissajous curves (solid lines) with contributions from elastic and viscous stress components (dotted lines)	46
Figure 3.17 – Example of LAOS data analysed using MITlaos	46
Figure 3.18 – Uniaxial deformation of material.....	47
Figure 3.19 – Typical transient extensional and shear viscosity of polymer solutions with time	48
Figure 3.20 – Schematic illustration of capillary breakup extensional rheometer	48
Figure 3.21 – Derivatisation of neutral monosaccharides into alditol acetates and TMS derivatives (adapted from Cui, 2005).....	51
Figure 3.22 – Illustration of a rat stomach (adapted from DeSesso & Jacobson, 2001).....	54
Figure 3.23 – Oral gavaging rats with mamaku gum	55
Figure 4.1 – Flow diagram of rheological techniques (shear and extensional) used to characterise the mamaku polysaccharide.....	57
Figure 4.2 – a) Viscosity curves of 2.5 (■), 3.5 (○), 5 (▲), 7 (▽) and 9% (◆) w/w native mamaku polysaccharide; b) representation of Newtonian, shear-thickening and shear-thinning regions on a viscosity curve.....	60
Figure 4.3 – Viscosity curves of 5% w/w mamaku obtained with various data collection time settings at 20°C 61	
Figure 4.4– a) Viscosity of 5% w/w mamaku as a function of time at various shear rates at 20°C ; b) magnified at 4 (●), 6 (○), 8 (▲) and 10s^{-1} (◇) during the first two minutes of the measurement	61
Figure 4.5 – Viscosity and first normal stress difference vs. shear rate for 2 and 10% w/w mamaku solutions at 20°C	63

Figure 4.6 – First normal stress difference (N_1) of 5% w/w mamaku with time at constant shear rates 4, 6, 8 and 10s ⁻¹ at 20°C	64
Figure 4.7 – Viscosity curves of 5% w/w mamaku on increasing (filled symbols) and decreasing (unfilled symbols) shear rates at 20°C; a) 0.1 to 1s ⁻¹ ; b) 0.1 to 5s ⁻¹ ; c) 0.1 to 10s ⁻¹ (additional ▲/△ symbols indicate viscosity with 5 minutes rest after the up-curve); d) 0.1 to 1000s ⁻¹	65
Figure 4.8 – Viscosity changes with time as a function of shear history of 1 (+), 10 (○) or 1000s ⁻¹ (△) of 5% w/w mamaku at 20°C; each symbol represents one data series sheared for a total of 80 minutes. For example, to test the effects of shear history at 1000s ⁻¹ (△/black symbols), the sample was sheared at 1000s ⁻¹ , followed by 1s ⁻¹ , and subsequently back to 1000s ⁻¹ , and then followed by 10s ⁻¹ , and again back to 1000s ⁻¹ then followed by 100s ⁻¹	66
Figure 4.9 – Viscosity changes with time as a function of pre-shear at 10s ⁻¹ for 5% w/w mamaku at 20°C; solid line represents viscosity of 5% w/w mamaku at 1s ⁻¹ from rest	66
Figure 4.10 – a) Frequency sweep ($\gamma_0 = 5\%$) and b) concentration dependence of relaxation time for 2.5, 5 and 7% w/w mamaku polysaccharide	69
Figure 4.11 – Superposition of apparent viscosity (η , filled symbols) obtained by steady-shear measurements and complex viscosity (η^* , unfilled symbols) obtained by oscillatory measurements for 2.5 (■), 5 (▲) and 7% (●) w/w mamaku solutions	70
Figure 4.12 – Amplitude sweep (G' (■), G'' (□) and δ (▲) as a function of % strain) of 10% w/w mamaku at $\omega = 10$ rad/s, 20°C	71
Figure 4.13 – a) Three-dimensional and b) two-dimensional Lissajous-Bowditch plots of stress vs. strain and c) stress vs. strain rate of 10% w/w mamaku at $\omega = 10$ rad/s from 0.1 to 3,000% strain, 20°C; The linear viscoelastic, strain-softening, strain-hardening and strain-softening regions are coloured green, yellow, red and brown respectively	73
Figure 4.14 – Elastic (stress vs. strain) Lissajous-Bowditch plots of 10% mamaku at $\omega = 10$ rad/s for a) LVER (region I, 0.6-10% γ_0 , green, dotted lines outline the overall ellipsoidal shape of the Lissajous plots); b) strain softening (region II, 20-800% γ_0 , yellow, clockwise arrow indicate inter-cycle strain-softening) ; c) strain-hardening (region III, 800-2000% γ_0 , red, anti-clockwise arrow indicates inter-cycle strain-hardening) and d) strain-softening (region IV, 2000-5010% γ_0 , brown); Examples of determining G'_M (minimum strain modulus, gradient of tangent at $\gamma_0 = 0$, solid line) and G'_L (maximum strain modulus, gradient of secant at γ_{max} , dashed line) are shown for each region	74
Figure 4.15 – Normalised elastic Lissajous curves (stress vs. strain) for 10% w/w mamaku solution arranged in a Pipkin space at $\omega = 1, 2.5, 5, 10$ rad/s and $\gamma_0 = 10, 631, 1580$ and 2510%. Maximum stress values are indicated at the top left corner of each Lissajous plot. The linear viscoelastic, strain-softening, strain-hardening and strain-softening regions are coloured green, yellow, red and brown respectively.	76
Figure 4.16 – a) Comparison of new LAOS parameters with original first-harmonic moduli; b) strain-stiffening and shear-thickening ratio of 10% w/w mamaku at 1-6000% strain amplitude	77
Figure 4.17 – Superposition of oscillatory measurements (G' vs. strain rate) on rotational measurements (η vs. shear rate) for a) 2.5% and b) 5% w/w mamaku	79

Figure 4.18 – Evolution of fluid filament diameter with time for a) 2.5, b) 5.0 and c) 7.0% w/w using CaBER; initial aspect ratio $\Lambda_0 = L_0/D_0 = 1.6/6 = 0.27$ and final aspect ratio $\Lambda = 7.4/6 = 1.23$; solid lines represent fitted data in the elasto-capillary regime using Equation 4.8; d) comparison between 2.5, 5.0 and 7.0% w/w on a log-scale with their respective relaxation times at 25°C.....	80
Figure 4.19 – Still frames of fluid filament during CaBER experiment at 25°C for a) 2.5% w/w (breakup time, $\tau_b=0.80s$) and b) 5.0% w/w ($\tau_b=55.3s$) at various times normalised by breakup time, \underline{t} , where $\underline{t}=t/\tau_b$	80
Figure 4.20 – Normalised diameter $D(t)/D_0$ plotted against non-dimensional time $\tau^* = t/\lambda$ where λ is the corresponding relaxation time of the three mamaku gum solutions	81
Figure 4.21 – a) Extensional viscosity and b) Trouton ratio of 2.5 (■) and 5% (●) w/w mamaku as a function of accumulated Hencky strain at 25°C.....	84
Figure 5.1 – Flow diagram for probing stability and intermolecular associations in mamaku polysaccharide	88
Figure 5.2 – Viscosity curves of a) 2.5% and b) 5 %w/w mamaku polysaccharide at 5 (■), 10 (●), 15 (▲), 20 (▼), 25 (◆), 30 (◀), 35 (▶), 40 (●), 45 (◆) & 50°C (★).....	92
Figure 5.3 – a) Dependence of peak viscosity, η_{max} (■) and characteristic time scale, $1/\gamma_{max}$ (●) on temperature for 5% w/w mamaku; b) characteristic time scale normalised by concentration (2.5 (■), 5 (○), 7 (▲) & 9% w/w (▼)) with temperature.....	93
Figure 5.4 – Reduced viscosity ($\eta_r=b_T \cdot \eta$) vs. reduced shear rate ($\gamma r=a_T \cdot \gamma$) of 5% w/w mamaku at various temperatures; inset: horizontal (a_T) and vertical (b_T) shift factors with temperature, $T_{ref}=20^\circ C$	94
Figure 5.5 – Time-temperature superposition of reduced storage modulus (G'_r) vs. reduced angular frequency ($\omega_r=a_T \cdot \omega$) of 5% w/w mamaku at various temperatures ($\gamma_0=5\%$); inset: horizontal shift factor (a_T) with temperature, $T_{ref}=20^\circ C$	94
Figure 5.6 – Arrhenius plots of critical (squares) and maximum (circles) viscosities (filled) and shear rates (unfilled) of 2.5% w/w mamaku	96
Figure 5.7 – Activation energies based on viscosity at critical (■), maximum (□), $0.1s^{-1}$ (●) and $1000s^{-1}$ (○) shear rates at different mamaku concentrations (% w/w)	96
Figure 5.8 – Viscosity curves of a) 2.5 and b) 5% w/w mamaku polysaccharide with 0 (■), 1 (●), 2 (▲), 3 (▼), 4 (◆) & 5M (◀) urea at 20°C.....	98
Figure 5.9 – a) Dependence of peak viscosity (η_{max}) (■) and characteristic time scale ($1/\gamma_{max}$) (●) on urea concentration for 5% w/w mamaku; b) inverse of maximum shear rate normalised by mamaku concentration (2.5 (■), 5 (○), 7% w/w (▲)) at 20°C.....	99
Figure 5.10 – Reduced viscosity ($\eta_r=b_C \cdot \eta$) vs. reduced shear rate ($\gamma r=a_C \cdot \gamma$) of 5% w/w mamaku with 0 (■), 1 (●), 2 (▲), 3 (▼), 4 (◆) and 5M (◀) urea; inset: horizontal (a_C ; ●) and vertical (b_C ; ○) shift factors with urea concentration, $C_{ref}=0M$ and 20°C	100
Figure 5.11 – Time-urea concentration superposition of frequency sweeps of 5% w/w mamaku with 0 (■), 1 (●), 2 (▲), 3 (▼), 4 (◆) and 5M (◀) urea by shifting along x-axis with shift factor, a_c ; inset: shift factor values with urea concentration, $C_{ref}=0M$ at 20°C.....	101
Figure 5.12 – Viscosity curves of 5% w/w native mamaku extract before (■) and after (▲) dialysis (MWCO 12-14,000 Da), and addition of 0.05M NaCl (●) for increasing (filled) and decreasing shear rates (unfilled symbols) at 20°C.....	102

Figure 5.13 – a) Effect of NaCl concentration (0.001 (×), 0.005 (+), 0.01 (*), 0.05 (●), 0.1 (▲), 0.25 (▼), 0.5 (◆) & 1.0M (◀) on shear-thickening of 5% w/w dialysed mamaku at 20°C; b) Zero-shear viscosity (■) estimated using a modified Cross' equation for shear-thickening fluids and viscosity at 100s-1 (○) at various NaCl concentrations	104
Figure 5.14 – a) Frequency sweeps G' (filled) and G'' (unfilled) of 5% w/w dialysed mamaku at 0 (■), 0.001 (●) & 0.05M (▶) NaCl at 1% strain and 20°C; b) relaxation time of dialysed mamaku with NaCl concentration (0.001-0.5M).....	106
Figure 5.15 – Effect of CaCl ₂ concentration (0.001 (×), 0.005 (●), 0.01 (▲), 0.05 (▼), 0.1 (◆), 0.25 (◀), 0.5 (▶) & 1.0M (●)) on shear-thickening of 5% w/w dialysed mamaku at 20°C.....	107
Figure 5.16 – Dialysed mamaku extract in (from left to right) 0.001-0.1M LaCl ₃ •7H ₂ O	108
Figure 5.17 – Effect of LaCl ₃ •7H ₂ O concentration (0.001 (×), 0.1 (+), 0.25 (●), 0.5 (▼), 0.75 (■) & 1.0M (◆)) on shear-thickening of 5% w/w dialysed mamaku; sample precipitation occurs with 0.005, 0.01, 0.05M LaCl ₃ •7H ₂ O at 20°C	108
Figure 5.18 – Effect of AlCl ₃ •6H ₂ O concentration (0.001 (×), 0.005 (+), 0.01 (*), 0.05 (▼), 0.1 (◆), 0.25 (◀), 0.5 (▶) & 1.0M (●)) on shear-thickening of 5% w/w dialysed mamaku at 20°C.....	109
Figure 5.19 – Effect of LaCl ₃ •7H ₂ O concentration on relative viscosity (■) of 1% w/w dialysed mamaku and zeta-potential (○) of 5% w/w dialysed mamaku at 20°C	109
Figure 5.20 – Viscosity curves of native (□) and dialysed (⊠) mamaku extract with salts of different cation valencies i.e. monovalent (NaCl (⊕), KCl (○), TMAC (⊙)), divalent (CaCl ₂ (◆), MgCl ₂ (⊠)) and trivalent (AlCl ₃ (△) (also at 0.01M (▲)), LaCl ₃ (▲)) at 0.1M concentration and 20°C	111
Figure 5.21 – Comparison of a) viscosity at critical shear rate, b) critical shear rate & c) extent of shear-thickening with various mono- (NaCl (⊕), KCl (□) , di- (CaCl ₂ (●), MgCl ₂ (○)) and trivalent (AlCl ₃ (▲), LaCl ₃ (△)) cations at equivalent ionic strengths (lines serve as visual guides)	113
Figure 5.22 – a) Viscosity curves of 5% w/w dialysed mamaku under various pH conditions (pH 1-11) and b) magnified in pH region from 2.0-5.0	114
Figure 5.23 – pKa titration curve of dialysed mamaku solution (5% w/w).....	114
Figure 6.1 – Flow diagram of overall purification scheme of mamaku extract	121
Figure 6.2 – Carboxyl reduction of methylesterified and non-methylesterified uronic acids (adapted from Pettolino, Walsh, Fincher, & Bacic, 2012)	125
Figure 6.3 – Summary of glycosyl linkage analysis based on methylation, hydrolysis, reduction and acetylation reactions (adapted from Pettolino, et al., 2012)	126
Figure 6.4 – Appearance of native mamaku solution before (left) and after (right) ultracentrifugation at 250,000g for 1 hour at 20°C.....	128
Figure 6.5 – Yield of solid material before and after ultracentrifugation (UC) and ethanol precipitation (EtOH)	128
Figure 6.6 – Protein removal using Sevag reagent; top brown layer: aqueous polysaccharide phase; water-chloroform interface: denatured protein gel; bottom clear layer: chloroform phase	129
Figure 6.7 – Extraction scheme for multiple ethanol precipitation of native mamaku polysaccharide solution	131
Figure 6.8 – Appearance of polysaccharide residue after first and second ethanol precipitations.....	132

Figure 6.9 – Viscosity curves of purified mamaku solutions (0.8% w/w) with one (EtOH x 1, ■) or two (EtOH x 2, ●) ethanol precipitations, and the alcohol-soluble fraction after two precipitations (E2, ○).....	133
Figure 6.10 - Molecular weight analysis by size-exclusion coupled with multi-angle laser light scattering (SEC-MALLS) of purified mamaku polysaccharide	135
Figure 6.11 – a) Viscosity curves of purified mamaku at concentrations of 0.2-1.4% w/w; dashed lines represent viscosity of a 5% w/w native mamaku solution before purification; b) Concentration dependence of zero-shear viscosity; Unfilled symbols (□) represent viscosities measured using an Ubbelohde dilution capillary viscometer; filled symbols (■) are zero-shear viscosities in the dilute regime estimated by fitting the Cross equation to the complex viscosity curves.....	136
Figure 6.12 – Selected regions of the a) ¹³ C-NMR and b) ¹ H-NMR spectra of purified mamaku polysaccharide	140
Figure 6.13 – Possible structure of mamaku polysaccharide; R = T-Xylp, T-Galp or T-GlcpA and other more complex oligosaccharides containing sugars with linkages shown in Table 6.4	141
Figure 7.1 – Summary of experimental design in a flow diagram	144
Figure 7.2 – Boxplot of stomach contents two hours after gavaging with 4ml mamaku or water; a significant difference (*) was found in the weight of contents remaining in the stomach of rats gavaged with mamaku compared with those gavaged with water; horizontal line represents the median and the box represents the interquartile ranges.....	147
Figure 7.3 – Mamaku gum removed from the stomach two hours post-gavage	147
Figure 7.4 – Mean quantity of food consumed by each treatment group from day 16 to day 24; red arrows indicate days which the rats have been gavaged; significant difference (*) between groups gavaged with mamaku and water on day 22 (3 rd gavage) and for all gavaging days (****) based on repeated measures ANOVA; bars represent standard error (SE) of the mean	148
Figure 7.5 – a) Cumulative average weight gain of mamaku and water group during gavaging week (day 17-26); error bars represent SE of the mean; red arrows indicate days which the rats have been gavaged; b) Average weight gain of mamaku and water group during acclimation (day 1-16), gavaging (day 17-25), and for the entire experiment (day 1-25).....	149
Figure 7.6 – Average weight gain after gavage (total weight change 24 hours after gavage e.g. weight difference between days 17 and 18) and between gavage (total weight change in 24 hours without gavage e.g. weight difference between days 18 and 19) gavages for mamaku and water group; significant difference (****) between groups gavaged with mamaku and water 24 hours after gavage based on repeated measures ANOVA error bars represent SE of the mean.....	149
Figure 7.7 – Illustration of the gastric emptying process (adapted from Sherwood, 1993)	151
Figure 7.8 – Viscosity curve of 15% w/w mamaku solution at 37°C	152
Figure 7.9 – Viscosity curves of 17% w/w mamaku gum and 1.5% w/w guar gum at 20°C.....	153
Figure 8.1 – Schematic illustration of the polysaccharide during shear and extensional deformations (dotted lines represent intermolecular hydrogen bonds)	159
Figure 8.2 – Schematic illustration of overview of effects of temperature, urea, cations and pH on the polysaccharide during shear	160
Figure 8.3 – Schematic illustration of purification and structural characterisation of the polysaccharide.....	161

Figure 8.4 – Schematic illustration of possible hydrogen bond configurations between functional groups in the polysaccharide chain responsible for hydrogen bonding 162

Figure 8.5 – Schematic illustration on effects of mamaku polysaccharide on the food intake, body weight and gastric emptying in rats..... 163

List of Tables

Table 2.1 – Plant polysaccharides of industrial significance and their sources and applications	4
Table 2.2 – Proximate and mineral composition of freeze-dried extract from the mamaku fronds (Goh, et al., 2007)	8
Table 2.3 – Molecular characteristics of the water-soluble extract from mamaku	8
Table 2.4 – Structural levels of polysaccharides (Walter, 1998)	9
Table 3.1 – Comparison between elastic solids and viscous liquids based on the spring and dashpot mechanical models (adapted from Trinh & Trinh, 2009)	37
Table 3.2 - Specifications for Paar Physica rheometer MCR-301	39
Table 4.1 – Zero-shear viscosity (η_0), surface tension (σ), extensional relaxation time (λ_E) and shear relaxation time (λ_s) of 2.5, 5.0 and 7.0% w/w mamaku solutions	81
Table 4.2 – Trouton ratios of various polymers	85
Table 5.1 – Activation energy of viscous flow (kJ/mol) for various polymers	97
Table 5.2 –Mineral composition of native and dialysed mamaku extract (mg/g NSP†)	103
Table 5.3 – Ionic and hydrated ionic radius of various cations	112
Table 6.1 – Protein content of purified mamaku obtained with protein removal using protease or Sevag's reagent determined using the Leco total combustion method	129
Table 6.2 – Comparison of chemical composition of native and purified mamaku fractions	134
Table 6.3 – Constituent sugar composition of purified mamaku polysaccharide determined using HPAEC and GC-MS	137
Table 6.4 – Glycosyl linkage composition of carboxyl-reduced mamaku polysaccharide	139

List of Publications

Based on the thesis:

1. Wee, M. S. M., Matia-Merino, L., Carnachan, S. M., Sims, I. M., Goh, K. K. T. (2014). Structure of a shear-thickening polysaccharide extracted from the New Zealand black tree fern, *Cyathea medullaris*. *International journal of biological macromolecules*, 70(0), 86-91.
2. Wee, M. S. M., Matia-Merino, L., Goh, K. K. T. (2015). Time and shear-history dependence of rheological properties of a water soluble extract from the fronds of the black tree fern, *Cyathea medullaris*. *Journal of Rheology*, 59, 365.
3. Wee, M. S. M., Matia-Merino, L., Goh, K. K. T. (accepted in Carbohydrate Polymers). Effect of cation concentration and valency on shear-induced thickening of mamaku polysaccharide.
4. Jaishankar, A., Wee, M. S. M., Matia-Merino, L., Goh, K. K. T., McKinley, G. H. (2015). Probing hydrogen bond interactions in a shear-thickening polysaccharide using nonlinear shear and extensional rheology. *Carbohydrate Polymers*, 123, 136-145.
5. Wee, M. S. M., Jaishankar, A., Matia-Merino, L., Goh, K. K. T., McKinley, G. H. (in preparation). Large amplitude oscillatory shear characterisation of a shear-thickening polysaccharide extracted from the New Zealand black tree fern, *Cyathea medullaris*.

Others

6. Wee, M. S. M., Nurhazwani, S., Tan, K. W. J., Goh, K. K. T., Sims, I. M., and Matia-Merino, L. (2014). Complex coacervation of an arabinogalactan-protein extracted from the *Meryta sinclairii* tree (puka gum) and whey protein isolate. *Food Hydrocolloids*, 42, 130-138.
7. Goh, K. K. T., Wee, M. S. M., and Hemar, Y. (2013). Phase stability-induced complex rheological behaviour of galactomannan and maltodextrin mixtures. *Food & Function* 4, 627-634.
8. Wee, M. S. M., Goh, K. K. T., Sims, I. M., and Matia-Merino, L. (in preparation). Rheological and molecular characterisation of an arabinogalactan-protein extracted from the *Meryta sinclairii* tree (puka gum).